JVSTA
JOURNAL OF VACUUM SCIENCE AND TECHNOLOGY A

Mechanisms for sealing of porous low-k SiOCH by combined He and NH3 plasma treatment

Juline Shoeb and Mark J. Kushner

Citation: J. Vac. Sci. Technol. A **29**, 051305 (2011); doi: 10.1116/1.3626534
View online: http://dx.doi.org/10.1116/1.3626534
View Table of Contents: http://avspublications.org/resource/1/JVTAD6/v29/i5
Published by the AVS: Science & Technology of Materials, Interfaces, and Processing

Related Articles

HfxZr1−xO2 compositional control using co-injection atomic layer deposition
J. Vac. Sci. Technol. A 31, 01A115 (2013)

Thin film high dielectric constant metal oxides prepared by reactive sputtering
J. Vac. Sci. Technol. B 30, 062202 (2012)

Investigation on spatially separated atomic layer deposition by gas flow simulation and depositing Al2O3 films
J. Vac. Sci. Technol. A 30, 051504 (2012)

Damage by radicals and photons during plasma cleaning of porous low-k SiOCH. I. Ar/O2 and He/H2 plasmas
J. Vac. Sci. Technol. A 30, 041303 (2012)

Remote H2/N2 plasma processes for simultaneous preparation of low-k interlayer dielectric and interconnect copper surfaces
J. Vac. Sci. Technol. B 30, 031212 (2012)

Additional information on J. Vac. Sci. Technol. A

Journal Homepage: http://avspublications.org/jvsta
Journal Information: http://avspublications.org/jvsta/about/about_the_journal
Top downloads: http://avspublications.org/jvsta/top_20_most_downloaded
Information for Authors: http://avspublications.org/jvsta/authors/information_for_contributors

ADVERTISEMENT

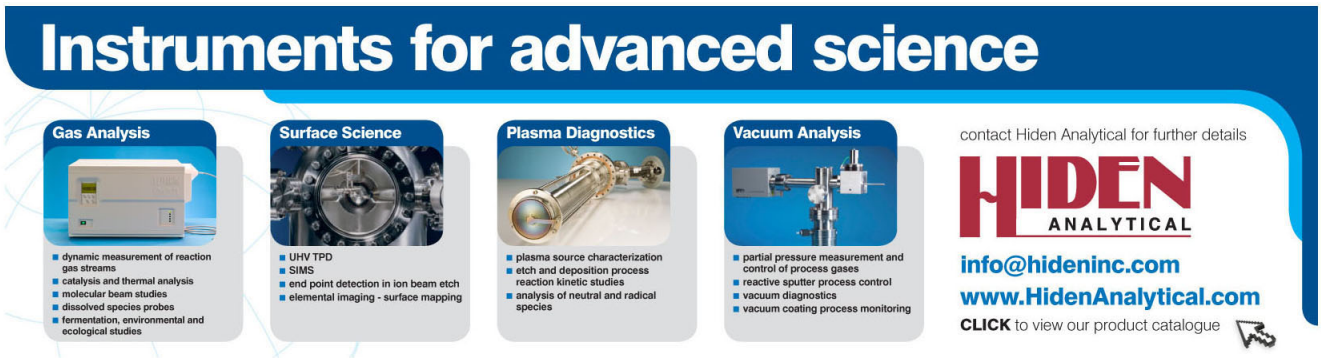

Mechanisms for sealing of porous low-*k* SiOCH by combined He and NH_3 plasma treatment

Juline Shoeb[a)]
Department of Electrical and Computer Engineering, Iowa State University, Ames, Iowa 50011

Mark J. Kushner[b)]
Department of Electrical Engineering and Computer Science, University of Michigan, Ann Arbor, Michigan 48109

(Received 2 June 2011; accepted 24 July 2011; published 22 August 2011)

Porous dielectric materials, such as SiOCH, are used as the insulator in interconnect wiring in microelectronics devices to lower the dielectric constant and so decrease the RC time delay. Sealing of the pores (up to a few nm in diameter) is necessary to prevent degradation of the *low-k* properties during subsequent processing steps by diffusion of reactants through the pores into the material. Sequential treatment of porous SiOCH by He and NH_3 plasmas is potentially a means of sealing pores while maintaining the *low-k* of the dielectric. The He plasma activates surface sites to accelerate the reactions responsible for pore sealing. NH_3 plasma treatment completes the sealing through one of two mechanisms resulting from the adsorption of NH_x radicals — catalyzing the formation of a densified surface layer or formation of Si-N, C-N and N-N bonds to bridge over the pore. In this paper, we discuss mechanisms for pore sealing bridging bonds based on results from an integrated computational investigation of the etching, cleaning, activation and sealing of porous SiOCH in sequential $Ar/C_4F_8/O_2$, Ar/O_2, He and Ar/NH_3 plasmas. The authors found that pores in excess of 1 nm in radius are difficult to seal due to the inability of N-bonding to bridge the pore opening. Factors affecting the sealing efficiency, such as treatment time, average pore radius and aspect ratio are discussed.
[DOI: 10.1116/1.3626534]

I. INTRODUCTION

Porous dielectric materials having a low dielectric constant (*low-k*) are being used to decrease the interconnect wiring capacitance to limit the *RC* time delay in integrated circuits.[1] SiOCH, silicon dioxide with CH_x groups lining the pores, is one commonly used material, having porosities as large as 50% with pore diameters of up to a few nm. The pores can also be interconnected, offering pathways for reactive species to enter into the porous network during plasma etching or cleaning steps.[1,2] Penetration by plasma produced radicals into the interior of the material is thought to compromise its *low-k* nature. These radicals can react with the CH_x groups to increase the average dielectric constant and so increase the *RC* time delay.

In order to maintain the *low-k* values of porous dielectrics, sealing of the pores at the surface may be necessary to prevent penetration of plasma produced species into the material during subsequent processing steps.[3–7] Dielectrics are typically etched in fluorocarbon plasmas in which there is deposition of a CF_x polymer. The residual CF_x polymer remaining at the end of the etch can, in fact, effectively seal the pores.[8] While CF_x polymers have good sealing characteristics because of their low dielectric constant and hydrophobic properties, the fluorine in the polymers creates compatibility issues with diffusion barriers including chemically active metals like Ti and Ta.[8] As a result, the CF_x polymer must be removed followed by a more integration compatible treatment for pore sealing.

The removal of the CF_x layer would ideally be performed using an oxygen containing plasma due to the efficiency of oxidation of the polymer by oxygen radicals.[9–11] Unfortunately, the underlying SIOCH film can also be damaged by the oxygen plasma, primarily by removing methyl groups by oxygen radicals which diffuse into the porous network.[12,13] This damage occurs in downstream effluents of oxygen containing plasmas at room temperature where ion energies are expected to be low and so is likely to be nearly a spontaneous process. Cleaning using oxygen containing plasmas is then a trade-off between treatments that are long enough to fully remove the CF_x polymer while not producing significant damage to the SiOCH.

Sequential treatment of SiOCH by He and NH_3 plasmas has been shown to seal pores without surface damage while maintaining the *low-k* nature of the SiOCH.[4–6] Pretreatment with He plasmas is thought to create active surface sites which localize and accelerate the chemical reactions responsible for pore sealing.[5,14] The processes whereby subsequent NH_3 plasma treatment completes the sealing are uncertain but at least two mechanisms have been proposed. The first proposes that NH_3 plasma treatment catalyzes pore collapse and so produces a dense nonporous layer at the surface.[6] The second proposes that chemisorption of NH_x radicals result in Si-N and C-N bonding which leads to bridging of the opening of the pores.[4,5,14] Recent experimental results favor the latter mechanism.[15]

[a)]Electronic mail: jshoeb@iastate.edu
[b)]Author to whom correspondence should be addressed; electronic mail: mjkush@umich.edu

In this paper, results from a computational investigation of pore sealing of *low-k* SiOCH, will be discussed on the basis of the bridging mechanism suggested in Refs 4 and 5, while varying porosity, interconnectivity, treatment time, pore radius, and aspect ratio. We modeled a fully integrated 4-step etch, clean, activation and pore sealing process. The sequence begins with etching of an 8:1 aspect ratio trench in porous SiOCH using an $Ar/C_4F_8/O_2$ capacitively coupled plasma (CCP). Residual CF_x polymers on the sidewalls of the SiOCH were then removed using an Ar/O_2 inductively coupled plasma (ICP). Subsequently a He ICP treatment followed by an Ar/NH_3 ICP treatment was applied to seal the pores open to the surface. We found that sealing efficiency is nearly independent of interconnectivity and porosity, but decreases with increasing pore radius due to the inability for pore-sealing N-bonding to produce long chains. The sealing efficiency in trenches is sensitive to the respective lengths of activation and sealing treatments due to the need for reactive species to deeply penetrate into the feature where view angles to the plasma are small. For this reason, sealing efficiency generally decreases with aspect ratio of the trench.

The reaction mechanisms for sealing are discussed in Sec. II, followed by a discussion of sealing efficiency in Sec. III. Our concluding remarks are in Sec. IV.

II. REACTION MECHANISMS

A reaction mechanism was developed for plasmas sustained in He and NH_3/Ar mixtures and their interactions with *low-k* porous SiOCH. The Hybrid Plasma Equipment Model (HPEM) was employed to obtain the energy and angular distributions for charged and neutral species incident onto the surface.[16] The sealing reaction mechanism was implemented in the Monte Carlo Feature Profile Module (MCFPM) with which the evolution of the *low-k* surfaces properties are predicted.[17–19] The MCFPM resolves the porous material with approximately atomic resolution. The cell size in this work is square with 0.4 nm x 0.4 nm dimensions, which is an effective radius of 0.2 nm. This value is smaller by about a factor of three than the smallest average pore radius considered in this investigation. The creation of pores in the MCFPM mesh is discussed in Refs. 20 and 21. The internal surfaces of the pores in SiO_2 were lined with a single layer of $-CH_3$ to approximate the structure of SiOCH.

A four step, integrated process was modeled – (1) Etching of SiOCH in a fluorocarbon CCP, (2) cleaning in an oxygen containing ICP, (3) activation in a He ICP and (4) sealing in an NH_3 containing ICP. The reaction mechanism for etching of SiO_2 in $Ar/C_4F_8/O_2$ plasmas is discussed in Refs. 18 and 20. For etching of SiOCH, we additionally included activation reactions wherein H is removed from the CH_3 groups lining the pores creating active sites. This increases the sticking coefficient of, for example, CF_x radicals resulting in polymerization. We also included the etching of the CH_3 group by O atoms. The polymer deposited on the sidewalls of the trench during the etch step was removed by Ar/O_2 ICP treatment, using the reaction mechanism discussed in Ref. 21. In addition, the CH_3 group is activated by ion bombardment and etched by the oxygen radicals and ions as CO/CO_2 during the etch step.

After the cleaning step, He plasma treatment of the SiO_2 and exposed CH_3 groups is thought to create activated sites that assist in pore sealing during a subsequent Ar/NH_3 plasma treatment.[4,5,14] He^+ and VUV photons (whose fluxes are also computed in the plasma equipment model) break Si-O bonds and remove H from CH_3 groups lining the pores to create the active sites. The bond breaking and site activation reactions are summarized as,

$$(He^+)_g + = SiO_2 \rightarrow = SiO\bullet + = O\bullet + He_g, \quad (1)$$

$$h\nu + = SiO_2 \rightarrow = SiO\bullet + = O\bullet, \quad (2)$$

$$(He^+)_g + = Si(CH_n) \rightarrow = Si(CH_{n-1})\bullet + H_g + He_g, \quad (3)$$

$$h\nu + = Si(CH_n) \rightarrow = Si(CH_{n-1})\bullet + H_g, \quad (4)$$

where $= M\bullet$ represents a surface bonded, free radical site, and the subscript g represents a gas phase species. It has been proposed that during He plasma pretreatment a surface densification process occurs which shrinks the openings to the pores which then enhances the sealing efficiency by the NH_3 plasmas.[14] This densification produces only a small increase in sealing efficiency, on the order of a few percent, and is less important for pores of 0.8–0.9 nm pore radius.[14,15] As such, densification effects have been excluded in the model for simplicity.

Following He plasma treatment, $NH_x (x = 1, 2)$ species created in an Ar/NH_3 plasma are chemisorbed at activated sites on SiOCH forming Si-N and C-N bonds.[4,5,22–24] Chemical reactions between NH_x radicals and activated Si sites produce compounds such as $Si\text{-}NH_x$ $(x = 1, 2)$, $= Si\text{-}NH\text{-}Si =$ and $SiNH_x\text{-}NH_y$.[4,5,22] For porous SiOCH, C-N bonding is also possible forming $CH_x\text{-}NH_y$ compounds which are important to bridging the pore openings.[4,5] The model treats these chemisorbed species as precursors to further adsorption of NH_x which form N-N bonds linking C or Si atoms from opposite pore walls. This N-N bonding results in; for example, $= Si(HN)\text{-}(NH)(CH_n)Si =$ bridging compounds across pores. These processes and their probabilities are summarized as,

$$\bullet (NH_x)_g + = SiO_n\bullet \rightarrow = SiO_n(NH_x) \quad p = 0.80 \quad (5)$$

$$\bullet (NH_x)_g + = Si(CH_n)\bullet \rightarrow = Si(CH_n)(NH_x) \quad p = 0.40 \quad (6)$$

$$\bullet (NH_x)_g + = SiO_n(NH_x) \rightarrow = SiO_n(NH_x) - (NH_y) \quad p = 0.90 \quad (7)$$

$$\bullet (NH_x)_g + = Si(CH_n)(NH_x) \rightarrow = Si(CH_n)(NH_x) - NH_y \quad p = 0{:}90. \quad (8)$$

As suggested in Ref. 22, NH_3 molecules are physisorbed at exposed active surface sites but have limited contributions to sealing.

The probabilities for both surface site activation and sealing reactions have been determined by extensive parameterization of the models to be qualitatively consistent with

experimental results available in the literature. Bounds of reaction probabilities are set based on thermodynamic properties and change in enthalpy of reaction, and within those bounds parameterization and comparison to experiments refine the mechanism. Some examples of works that guided the development of the reaction mechanism follow.

It has been reported that a 20s He plasma treatment followed by a 20s NH_3 plasma treatment can essentially completely seal a porous *low-k* flat surface with 0.8 nm pore radius.[4,14] We parameterized the activation probabilities to determine those values that achieved nearly 100% activation and sealing on flat surfaces for similar fluences of radicals and ions. Si-O bond scission by photons has been reported by Urbanowicz *et al.*[14] Since the Si-O bond strength is larger than for C-H bond, it is expected similar processing conditions will also produce C-H bond cleavage, and so we included these processes. In this regard, H removal from CH_x groups along with Si-O bond scission during He plasma treatment of SiOCH has been reported by Dultsev *et al.*[5] It has been reported that an increase in power for He pretreatment more efficiently blocks water adsorption from air after NH_3 sealing, which indicates He^+ may play a role in activation that results in a better sealing.[4] We therefore included He^+ knock-on collisions which sputter H from Si-CH_x groups, and used a large substrate bias. Such high energy ions also produce Si-O bond scission. Although other bond-scissions may occur by He^+ and VUV fluxes, we chose to limit the reaction mechanisms to Si-O and H removal as being representative of those processes. Our model for N-C bonding was based on analogy to gas phase reactions.[5,22,25]

Operationally, the HPEM is first sequentially run four separate times with the etch, clean, passivation and sealing chemistries to produce fluxes of ions and radicals to the substrate for each of the processing steps. The MCFPM is then sequentially executed using these four sets of fluxes. The initial conditions for the first etch step is the masked but otherwise untreated SiOCH. The ending conditions from the MCFPM from the etch step are then used as the initial conditions for the clean step. This sequence is repeated for the activation and sealing steps. Each result for sealing efficiency discussed here is the average of 20 integrated processing sequences (80 MCFPM runs) where the initial distributions for pore size and distribution are determined by the choice of a different random number seed, as discussed in Refs. 20 and 21.

The first etch step was performed using a CCP sustained in $Ar/C_4F_8/O_2 = 80/15/5$, 40 mTorr, and powered at 10 MHz. The remaining steps were performed in an ICP reactor treating a wafer 15 cm in diameter. The coil was powered at 13.56 MHz with a 10 MHz bias on the substrate. The reactor was 26 cm in diameter with a wafer-to-coil height of 10 cm. The conditions for the polymer removal step were $Ar/O_2 = 5/95$, 10 mTorr, 100 sccm with 300 W ICP power. He treatment was also at 10 mTorr and 300 W. The ion density for the Ar/O_2 plasma was 2.6×10^{10} cm^{-3} and 3.8×10^{10} cm^{-3} for the He plasma. For both plasmas, a 250 V rf bias, produced ions incident on the substrate with average energy near 400 eV and with an angular spread from the vertical of $<15^0$. For the sealing step, the process conditions were 10 mTorr of $Ar/NH_3 = 25/75$ and 300 W. No substrate bias was applied. NH_4^+ had the highest ion density (2.9×10^{10} cm^{-3}), followed by NH_3^+ (2.6×10^{10} cm^{-3}). The major radical densities were NH_2 (2.4×10^{13} cm^{-3}) and NH (1.6×10^{13} cm^{-3}). The flux of NH_2 was 4×10^{17} $cm^{-2}s^{-1}$ and that of NH was 2×10^{16} $cm^{-2}s^{-1}$.

In the discussion that follows, we characterize the sealing process using *sealing efficiency*, η. The sealing efficiency is the fraction of pores that were initially open to the plasma that are sealed. η was determined for each set of conditions by running twenty separate simulations while varying the random number seeds that determine the geometrical layout of the pores and the random fluxes striking the substrate. The fractions of pores that are sealed are then averaged over these trials to produce η.

The measure of what is a good or acceptable sealing efficiency is ultimately determined by the subsequent processing steps and procedures. For example, water exposure of porous SiOCH produces Si-OH bonding which increases the dielectric constant k of the material. A good sealing efficiency might then be defined as the value that will prevent water during air exposure from entering the pores and increasing the k value. Ideally a sealing efficiency of 100% will prevent such damage. However, even partial sealing that reduces the average pore opening size will reduce water uptake by the porous network. In our own computational studies, we have found that $\eta > 70\%$ is effective at reducing water vapor uptake when porous SiOCH is exposed to humid air. With the caveat that the goodness of sealing is determined by the subsequent process steps, for purposes of discussion in this paper, $\eta \geq 70\%$ is likely a good criterion for acceptable sealing.

III. SEALING EFFICIENCY

The base case conditions for this study used an average pore radius in the SiOCH of 0.8 nm with a standard deviation of 0.1 nm. Both the porosity and interconnectivity were 30%. These parameters correspond to a k-value of about 2.5. $-CH_3$ groups line the pores of otherwise SiO_2 material, where CH_3 groups are connected to Si atoms. A typical region of the SiOCH (as represented in the MCFPM) at the top of the feature with an open pore is shown in Fig. 1(a). The entire feature after the four integrated steps is shown in Fig. 2: 2(a) after fluorocarbon plasma etching, 2(b) after removal of the polymer, 2(c) after hard mask removal and He plasma activation, and 2(d) after Ar/NH_3 plasma sealing. A typical pore after He plasma treatment is shown in Fig. 1(b) during which surface sites were activated by fluxes of He^+ and VUV photons. The pore after sealing by the Ar/NH_3 plasma is shown in Fig. 1(c). The pore openings were bridged by a short chain of, for example, Si-N-N-Si, C-N-N-C or Si-N-N-C bonding, thereby sealing the pore.

After plasma etching, a CF_x polymer layer about 1.5 nm thick remains on the surface of the SiOCH. The length of the Ar/O_2 plasma cleaning is a compromise between fully

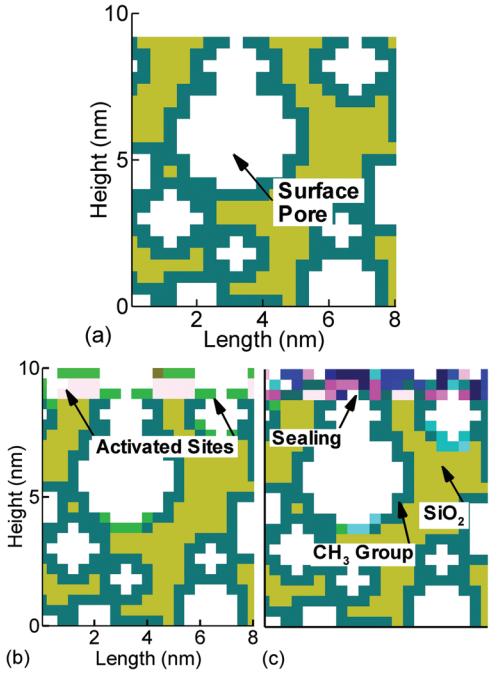

FIG. 1. (Color) Activation of pores open to the surface by He plasmas and sealing by Ar/NH_3 plasmas. (a) Typical initial conditions with CH_3 groups lining pores in SiO_2, an approximation to SiOCH. (b) Activated surface sites following He plasma treatment. (c) Sealed pores following Ar/NH_3 plasma treatment.

removing the CF_x polymer (longer times) and minimizing the removal of the $-CH_3$ groups by penetration of O atoms into the porous network (shorter times). Some residual CF_x remains in this tradeoff while a few pores have been opened or expanded by etching of their $-CH_3$ groups. Since activation by the He plasma is largely line-of-sight by directional photons and ions, the sidewalls of the trench are activated slowly compared to the top surfaces, and the interior surfaces of open pores are often not activated. After the sealing step, there is $-NH_x$ functionalization on all exposed surfaces whose sites were activated by the He plasma to saturation.

The purpose of the He plasma is to create reactive sites that are amenable to chemisorption by NH_x ($x = 1,2$). Site activation consists of loss of an H atom if the site is occupied by a $-CH_x$ group or Si-O bond breaking if the site is SiO_2. The fraction of surface sites that are activated by He^+ and photons is shown in Fig. 3 as a function of time of He plasma treatment. Results are shown for different probabilities of bond breaking per incident He^+ ion. For probabilities from 0.01 to 0.9, there is initially a rapid activation of sites corresponding to those that have direct view angles to the plasma. After this initial activation there is a slower asymptotic approach to activation of all sites that have any view angle to the plasma. Sites that are shadowed from direct line of site to the plasma due to the roughness of the porous surface must rely upon favorable reflection and backscatter of hot atoms for activation. Although the majority of surface sites can be activated on the top surface, within the trench, the smaller view angle to the plasma combined with shadowing by surface roughness allows a maximum of 80% surface

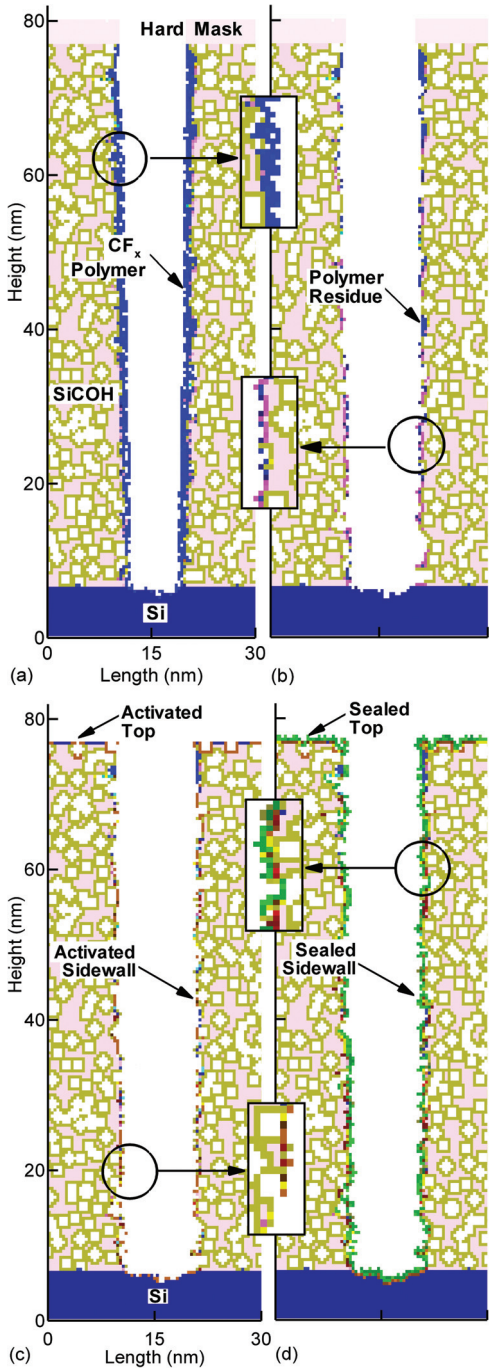

FIG. 2. (Color) Profiles of porous *low-k* SiOCH during integrated etch, clean, activation and sealing of an 8:1 aspect ratio trench. (a) After Ar/C_4F_8/O_2 plasma etching where sidewalls are covered with fluorocarbon polymers. (b) CF_x polymers are removed from sidewalls by Ar/O_2 plasma cleaning. (c) He plasma activated porous surfaces by Si-O bond breaking and H removal from CH_3 group. (d) Surface pores are sealed in Ar/NH_3 plasmas by NH_x adsorption at reactive surface sites forming Si-N and C-N bonds. (Color coding: dark pink — SiO_2, light pink — hard mask, olive — CH_3 groups, blue-CF_x polymer, brown — activated sites, green – N-containing bridging compounds.)

sites to be activated. High probabilities for activation, for example, $p = 0.8$ and 0.9 in Fig. 3, asymptote to this same value.

An interesting situation occurs when site activation for $p = 0.1$ is higher than that for $p = 0.2$ at times <50 s, as shown in Fig. 3. This is likely a consequence of the higher

reaction probability initially producing additional surface roughness which then shadows adjacent sites. However, as the activation time increases, the increase in probability of site activation dominates over the shadowing caused by the small increase in surface roughness.

η (the fraction of all pores open to the surface that are sealed) as a function of He plasma treatment time is shown in Fig. 4(a) for 30 s of Ar/NH_3 plasma treatment. Typical profiles with bridging sealing groups displayed are shown in Fig. 5. Without He plasma pretreatment, some activation of surface sites is accomplished by the Ar/NH_3 plasma and so some sealing does occur. However, the efficiency of activation is small compared to He plasmas and only 40% of the pores are ultimately sealed. For a flat *low-k* surface, as on the top of the surface of the feature, η increases with He plasma treatment time for up to 10 s as an increasing fraction of the Si-O surface bonds are broken and H is removed from surface $-CH_3$ groups. η then saturates when at about 95% when the majority of Si-O bonds and $-CH_3$ sites have been activated.

For the interior sidewalls of the trench, a longer He plasma time is required to activate sites deep in the trench to enable sealing. For instance, a 200 s He plasma pretreatment followed by a 30 s Ar/NH_3 plasma treatment seals 75% of the surface pores on the 8:1 aspect ratio trench sidewalls [shown in Figs. 2(d), 5(b) and 6(b)]. Overall η, which combines both flat surface and sidewall sealing, is 82%. The surface sites on sidewalls deeper in the trench require more time to be activated due to their smaller view-angles to the plasma. This dependence on depth in the trench is most critical for the directed or line-of-sight fluxes (ions and photons) which activate the surface sites. The passivating neutral NH_x neutral fluxes are less sensitive to view-angle to the plasma as there will be some diffusive reflection off the sidewalls; however these fluxes may be depleted by reactions as they diffuse into the trench.

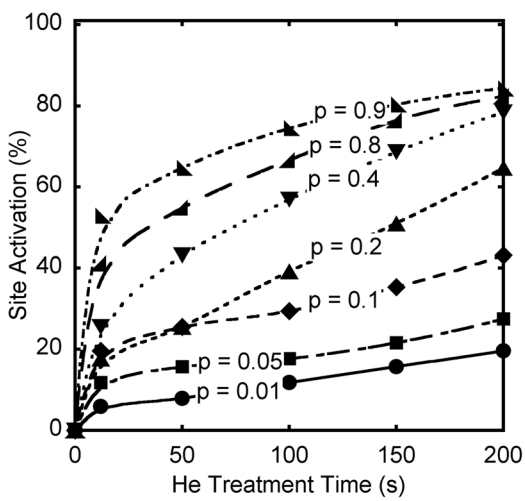

FIG. 3. Fraction of surface sites in a HAR trench activated in a He plasma as a function of treatment time. Values are shown for different probabilities for site activation by He^+ ion impact. The small view angle to the plasma and sites shadowed by surface roughness limits the percentage of sidewall surface sites that can be activated to about 80%. A higher surface activation probability reaches this saturated value faster but does not change the asymptotic value.

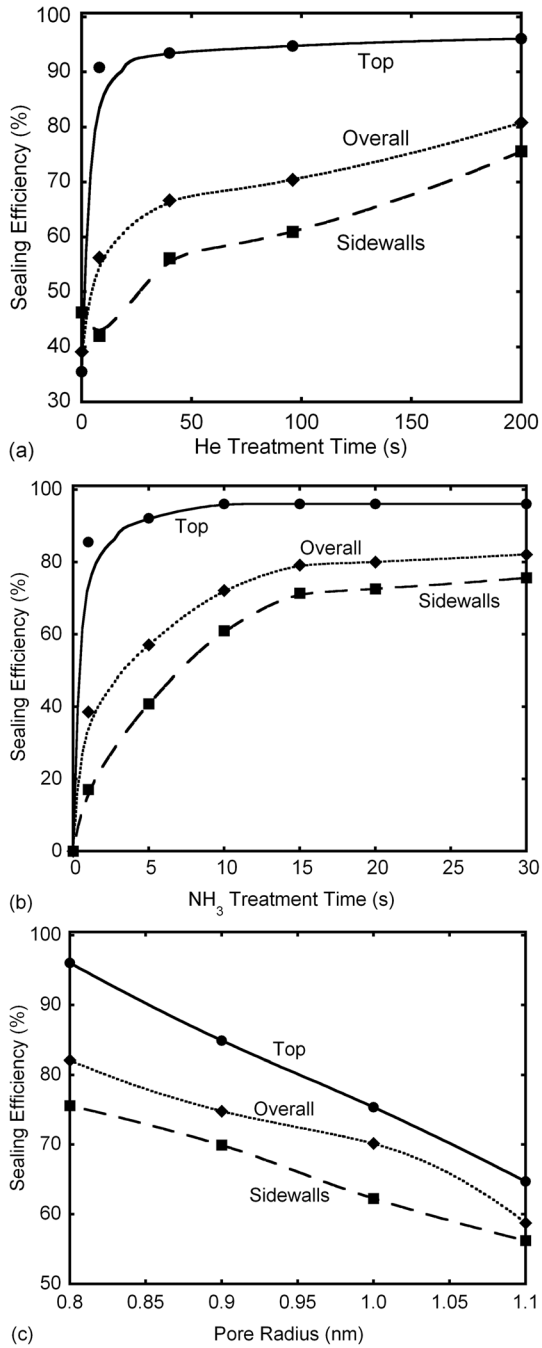

FIG. 4. Sealing efficiency as a function of (a) He plasma exposure time, (b) Ar/NH_3 plasma exposure time and (c) pore radius. For both surface site activation and sealing efficiency, sidewalls require more time for sealing due to their smaller view angle to the plasma and ultimately have a lower asymptotic value. Sealing efficiency decreases with increasing pore radius as the N-N bonding has a limited extent.

η as a function of Ar/NH_3 plasma treatment time is shown in Fig. 4(b) for 200 s of He plasma pretreatment. Ignoring the possibility of densification during He plasma treatment, in the absence of the Ar/NH_3 plasma treatment, there is no sealing. Sealing efficiency increases for the first 10 s on flat surfaces and for the first 20 s on trench sidewalls, and then saturates as the majority of the activated sites are passivated.

It takes a longer time for NH_x radicals to passivate the active sites on sidewalls deep inside the trench compared to the flat top surface due to the smaller view-angle to the plasma, achieving only 75% sealing.

The lower fraction of sealed sites on the sidewalls is more a function of the lack of activation by the He plasma than the inability of NH_x radicals to reach a site. For example, the sidewall sealing efficiency η was computed as a function of the length of NH_3 plasma treatment for short (8 s) and long (200 s) He plasma pretreatment times. The results are shown in Fig. 5 along with profiles for the two cases. In both cases, η first increases and then saturates as the NH_3 plasma treatment time increases. The short pretreatment time results in incomplete activation and η asymptotes to about 42%. The longer pretreatment time, able to activate more sites lacking direct view angles to the plasma, asymptotes to a higher sealing efficiency, about 75%. The incomplete sealing is shown by the profile in Fig. 5(a) where larger pores, lacking activated sites along the edges of the pore, are left open. The otherwise identical profile having longer He plasma pretreatment, has many of these larger pores sealed over.

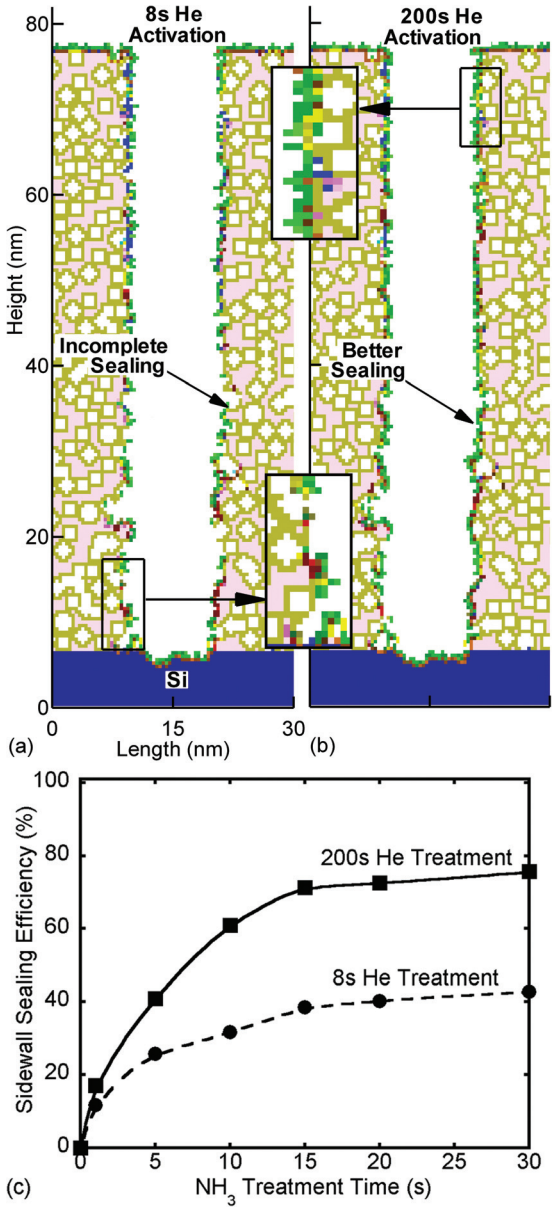

FIG. 5. (Color) Effect of He pretreatment time on sidewall sealing. Profiles of the trench after Ar/NH_3 sealing for He pretreatment time of (a) 8 s and (b) 200 s. (c) Sealing efficiency as a function of NH_3 plasma treatment time after 8 s and 200 s of He pretreatment. As the He pretreatment time increases the sealing efficiency as a function of NH_3 plasma treatment time saturates to a higher value. (Color coding: dark pink — SiO_2, olive — CH_3 groups, blue-CF_x polymer, brown — activated sites, green — N-containing bridging compounds.)

The sealing efficiency decreases with increasing pore size as shown in Fig. 4(c). Since NH_x compounds do not form long chains, sealing relies on the formation of C-N, Si-N and single N-N bonds to bridge the pore opening. The limited range for the bonding of these surface species sets the maximum pore size that can be sealed. Overall η decreases nearly linearly with pore size, to below 60%, as the pore radius exceeds 1.1 nm. These results are somewhat skewed by the persistence of a small amount of CF_x polymer on the sidewalls that provides about 5–10% of sealing (which does not occur on the top surface). This is due to the afore-mentioned limited exposure to Ar/O_2 cleaning plasmas to minimize the likelihood of removing $-CH_3$ groups. These results are also sensitive to the standard deviation of the distribution of the pore radii. Larger standard deviations for a given pore radius have a higher proportion of pores larger than the critical pore size that can be sealed. The end result is less sealing of those pores for the same average pore size. These trends are shown in Fig. 6 where profiles are shown of sealed SiOCH for different aspect ratios. Small pores or pores with a limited opening are efficiently sealed. Statistically larger pore openings cannot be bridged.

The activation of surface sites generally decreases with depth into the trench due to the decreasing view angle to the plasma. Truly shadowed features are not activated by photons — whereas such shadowed features are only activated by reflected hot neutrals of ions. As a result of this depth dependence, we found that for same He and Ar/NH_3 plasma treatment times, the sealing efficiency η on the sidewalls is inversely proportional to the trench aspect ratio as shown in Fig. 6(d). For example, with a smaller aspect ratio of 4, similar He and Ar/NH_3 plasma treatments sealed 90% of sidewall surface pores. For a larger aspect of 15, less than 50% of the sidewall pores were sealed.

We found that η is nearly independent of porosity and interconnectivity for a constant pore radius. With higher porosity for a fixed pore radius, the number of surface pores increases but the likelihood of sealing any given pore depends dominantly on its radius. A longer time may be required to seal the pores with increasing porosity but the final fraction of pores being sealed is the same. For a fixed porosity, increasing connectivity in principle only affects the geometrical relationship of pores to each other but should not affect the radii of individual pores. As a result, η is not sensitive to connectivity.

It has been experimentally shown that flat porous SiOCH having 0.8–0.9 nm pore radii can be completely sealed by combined He and NH_3 plasma treatment.[14] Our results for a flat *low-k* surface predict that such combined treatment

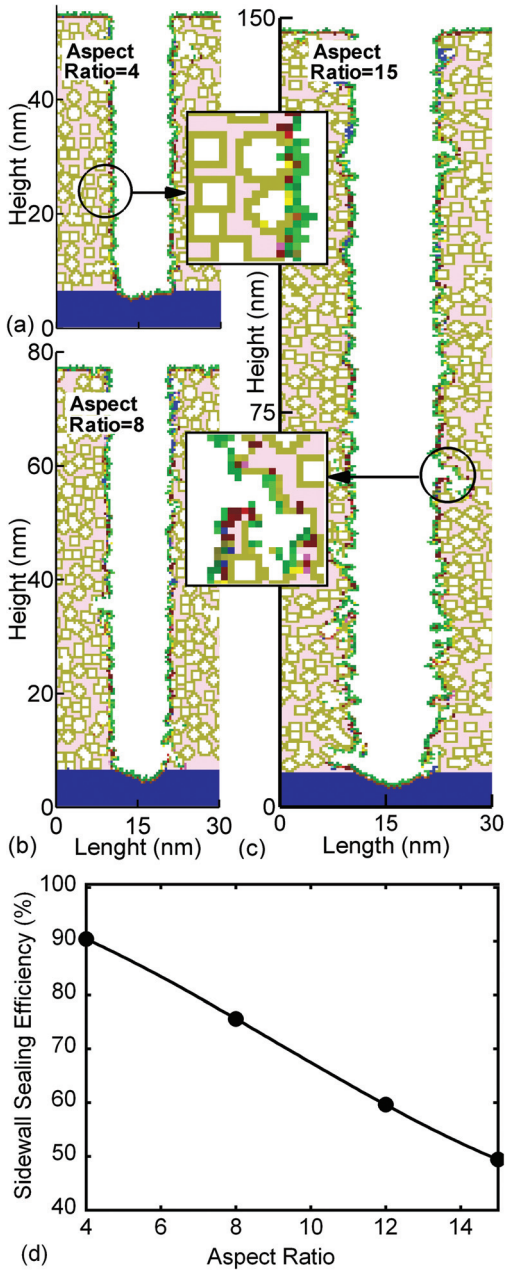

FIG. 6. (Color) Effect of aspect ratio effect on pore sealing. Profiles of trench after Ar/NH_3 plasma sealing for aspect ratios of (a) 4:1, (b) 8:1, and (c) 15:1. (d) Sealing efficiency as a function of aspect ratio. With equal times for He activation and NH_3 sealing, sidewall sealing efficiency is inversely proportional to the trench aspect ratio. (Color coding: dark pink — SiO_2, light pink — hard mask, olive — CH_3 groups, blue-CF_x polymer, brown — activated sites, green — N-containing bridging compounds.)

provides a sealing efficiency of >95%. Although our process conditions are different than reported in the literature, the scaling laws are generally applicable. Sealing of pores in SiOCH can be achieved by pretreating with He plasmas having sufficient VUV and He^+ fluences to activate sites, and treating with Ar/NH_3 plasmas having sufficient NH_x radical fluences to passivate the activated sites. This assumes that pore radii are not too large (generally $\leq$1 nm) and substrate biases are sufficiently low during the sealing step that -CH_x-NH_y and -Si-NH_x sealing compounds are not sputtered by energetic ions. As discussed in Refs. 4 and 5, if bridging is the dominant sealing mechanism, the bridging network will have a limited extent, and there should be a sensitivity of η on pore radius, as our results have shown. It has also been suggested that the small coverage of -NH_x groups responsible for pore sealing reside only on the surface and so are not likely to dominate IR absorption spectra.[4] In our model, only 1–2 monolayers of -NH_x radicals are adsorbed on the *low-k* which either bridge pore openings or form Si-NH_y/CH_x-NH_y compounds.

IV. CONCLUDING REMARKS

Integrated processing of high aspect ratio trenches in porous SiOCH using $Ar/C_4F_8/O_2$ plasmas for etching, Ar/O_2 plasmas for polymer removal, and successive He and NH_3 plasma treatments for activation and pore sealing were computationally investigated. To avoid diffusion of O species into the porous network which would remove –CH_3 groups, limited Ar/O_2 plasma exposure time was allowed, which resulted in traces of polymer to persist on the sidewalls. However, with He pretreatment these polymer sites were activated, enabling the polymer traces to be covered by C-N compounds during Ar/NH_3 sealing. Pore sealing was achieved by formation of Si-N and C-N bonds at He plasma activated sites followed by one N-N bond linking C or Si atoms from opposite pore walls. Pore sealing efficiency is nearly independent of porosity and interconnectivity, while being dependent on He and NH_3 plasma treatment time, pore radius, and aspect ratio. The efficiency of pore sealing decreases with increasing pore size due to the limited extent of these bonding configurations.

ACKNOWLEDGMENTS

This work was supported by the Semiconductor Research Corp. We acknowledge and sincerely thank A.M. Urbanowicz of IMEC, Belgium for useful discussions.

[1]C. M. Whelan, Q. T. Le, F. Cecchet, A. Satta, J. J. Pireaux, P. Rudlof, and K. Maex, Electrochem. Solid-State Lett. **7**, F8 (2004).
[2]G. Beyer, A. Satta, J. Schuhmacher, K. Maex, W. Besling, O. Kilpela, H. Sprey, and G. Tempel, Microelectron. Eng. **64**, 233 (2002).
[3]T. Abell and K. Maex, Microelectron. Eng. **76**, 16 (2004).
[4]A. M. Urbanowicz, D. Shamiryan, A. Zaka, P. Verdonck, S. De Gendt, and M. R. Baklanov, J. Electrochem. Soc. **157**, H565 (2010).
[5]F. N. Dultsev, A. M. Urbanowicz, and M. R. Baklanov, Mater. Res. Soc. Symp. Proc. **1079**, N07-03 (2008).
[6]H.-G. Peng, D.-Z. Chi, W.-De Wang, J.-H. Li, K.-Y. Zeng, R. S. Vallery, W. E. Frieze, M. A. Skalsey, D. W. Gidley, and A. F. Yee, J. Electrochem. Soc. **154**, G85 (2007).
[7]K. Hamioud, V. Arnal, A. Farcy, V. Jousseaume, A. Zenasni, B. Icard, J. Pradelles, S. Manakli, Ph. Brun, G. Imbert, C. Jayet, M. Assous, S. Maitrejean, D. Galpin, C. Monget, J. Guillan, S. Chhun, E. Richard, D. Barbier, and M. Haond, Microelectron. Eng. **87**, 316 (2010).
[8]G. Mannaert, M. R. Baklanov, Q. T. Le, Y. Travaly, W. Boullart, S. Vanhaelemeersch, and A. M. Jonas, J. Vac. Sci. Technol. B **23**, 2198 (2005).
[9]H. Seo, S. B. Kim, J. Song, Y. Kim, H. Soh, Y. C. Kim, and H. Jeon, J. Vac. Sci. Technol. B **20**, 1548 (2002).
[10]K. Sakuma, K. Machida, K. Kamoshida, Y. Sato, K. Imai, and E. Arai, J. Vac. Sci. Technol. B **13**, 902 (1995).
[11]M. A. Hartney, D. W. Hess, and D. S. Soane, J. Vac. Sci. Technol. B **7**, 1 (1989).

[12]D. Shamiryan, M. R. Baklanov, S. Vanhaelemeersch, and K. Maex, J. Vac. Sci. Technol. B **20**, 1923 (2002).
[13]O. V. Braginsky, A. S. Kovalev, D. V. Lopaev, E. M. Malykhin, Yu. A. Mankelevich, T. V. Rakhimova, A. T. Rakhimov, A. N. Vasilieva, S. M. Zyryanov, and M. R. Baklanov, J. Appl. Phys. **108**, 073303 (2010).
[14]M. Urbanowicz, M. R. Baklanov, J. Heijlen, Y. Travaly, and A. Cockburn, Electrochem. Solid-State Lett. **10**, G76 (2007).
[15]M. Urbanowicz, IMEC, Belgium, personal communication (13 January 2011).
[16]M. J. Kushner, J. Phys. D **42**, 194013 (2009).
[17]A. Agarwal and M. J. Kushner, J. Vac. Sci. Technol. A **27**, 37 (2009).
[18]D. Zhang and M. J. Kushner, J. Vac. Sci. Technol. A **19**, 524 (2001).
[19]J. Lu and M. J. Kushner, J. Vac. Sci. Technol. A **19**, 2652 (2001).
[20]A. Sankaran and M. J. Kushner, J. Vac. Sci. Technol. A **22**, 1242 (2004).
[21]A. Sankaran and M. J. Kushner, J. Vac. Sci. Technol. A **22**, 1260 (2004).
[22]J. L. Bischoff, F. Lutz, D. Bolmont and L. Kubler, Surf. Sci. **251**, 270 (1991).
[23]H.-W. Guo, L. Zhu, L. Zhang, S.-J. Ding, D. W. Zhang, R. Liu, Microelectron. Eng. **85**, 2114 (2008).
[24]S. Behera, J. Lee, S. Gaddam, S. Pokharel, J. Wilks, F. Pasquale, D. Graves, and J. A. Kelber, Appl. Phys. Lett. **97**, 034134 (2010).
[25]M. S. Foster, A. D. Williamson, and J. L. Beauchamp, Int. J. Mass Spactrom. Ion Phys. **15**, (429) 1974.